DTIC FILE COPY

CRREL REPORT 88-14

AD-A201 045

US Army Corps of Engineers
Cold Regions Research & Engineering Laboratory

On the pressure drop through a uniform snow layer

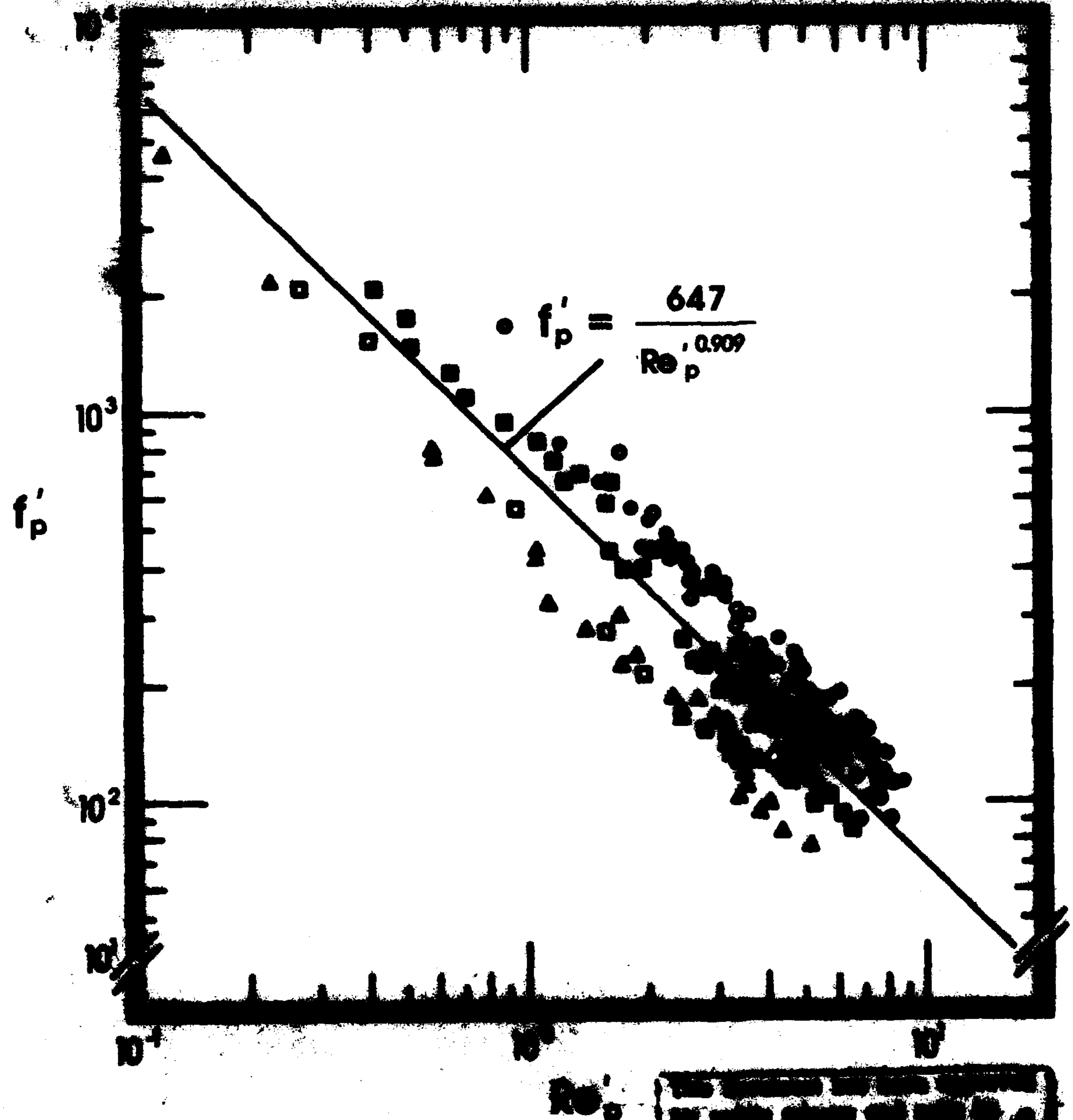

For conversion of SI metric units to U.S./British customary units of measurement consult ASTM Standard E380, Metric Practice Guide, *published by the American Society for Testing and Materials, 1916 Race St., Philadelphia, Pa. 19103.*

Cover: Relationship between friction factor f'_p and Reynolds number Re'_p (see Fig. 4).

CRREL Report 88-14

September 1988

On the pressure drop through a uniform snow layer

Yin-Chao Yen

QUALITY INSPECTED 2

Accession For		
NTIS GRA&I		X
DTIC TAB		☐
Unannounced		☐
Justification		
By		
Distribution/		
Availability Codes		
Dist	Avail and/or Special	
A-1		

Prepared for
OFFICE OF THE CHIEF OF ENGINEERS

88 1122 024

REPORT DOCUMENTATION PAGE

Form Approved
OMB No 0704-0188
Exp. Date Jun 30, 1986

1a. REPORT SECURITY CLASSIFICATION
Unclassified

1b. RESTRICTIVE MARKINGS

2a. SECURITY CLASSIFICATION AUTHORITY

2b. DECLASSIFICATION / DOWNGRADING SCHEDULE

3. DISTRIBUTION / AVAILABILITY OF REPORT
Approved for public release; distribution is unlimited.

4. PERFORMING ORGANIZATION REPORT NUMBER(S)
CRREL Report 88-14

5. MONITORING ORGANIZATION REPORT NUMBER(S)

6a. NAME OF PERFORMING ORGANIZATION
U.S. Army Cold Regions Research and Engineering Laboratory

6b. OFFICE SYMBOL (If applicable)
CECRL

7a. NAME OF MONITORING ORGANIZATION
Office of the Chief of Engineers

6c. ADDRESS (City, State, and ZIP Code)
Hanover, New Hampshire 03755-1290

7b. ADDRESS (City, State, and ZIP Code)
Washington, D.C. 20314-1000

8a. NAME OF FUNDING / SPONSORING ORGANIZATION

8b. OFFICE SYMBOL (If applicable)

9. PROCUREMENT INSTRUMENT IDENTIFICATION NUMBER

8c. ADDRESS (City, State, and ZIP Code)

10. SOURCE OF FUNDING NUMBERS

PROGRAM ELEMENT NO.	PROJECT NO	TASK NO	WORK UNIT ACCESSION NO
6.11.02A	4A1611 02AT24	SS	021

11. TITLE (Include Security Classification)
On the Pressure Drop Through a Uniform Snow Layer

12. PERSONAL AUTHOR(S)
Yen, Yin-Chao

13a. TYPE OF REPORT

13b. TIME COVERED
FROM ________ TO ________

14. DATE OF REPORT (Year, Month, Day)
September 1988

15. PAGE COUNT
18

16. SUPPLEMENTARY NOTATION

17. COSATI CODES

FIELD	GROUP	SUB-GROUP

18. SUBJECT TERMS (Continue on reverse if necessary and identify by block number)
Fluid flow
Friction coefficient
Porous media
Pressure
Snow

19. ABSTRACT (Continue on reverse if necessary and identify by block number)

An experimental study covering a mass flow rate ranging from 1.62 to 67.45 g/cm^2-s and snow density varying from 0.377 to 0.472 g/cm^3 has been conducted. Pressure drops ranging from 0.012 to 2.868 gf/cm^2 were recorded. A plot of the friction factor f_p vs Re_p (defined as the classical Reynolds number Re for fluid flow through conduits) showed a good representation of all the experimental data. The least-squares analysis resulted in an expression of $f_p = 118/Re_p^{1.095}$ for snow, in comparison with the expression $f_p = 64/Re_p$ developed for fluid flow through porous media of randomly packed metallic and nonmetallic materials of spherical and nonspherical shapes.

20. DISTRIBUTION / AVAILABILITY OF ABSTRACT
☒ UNCLASSIFIED/UNLIMITED ☐ SAME AS RPT. ☐ DTIC USERS

21. ABSTRACT SECURITY CLASSIFICATION
Unclassified

22a. NAME OF RESPONSIBLE INDIVIDUAL
Yin-Chao Yen

22b. TELEPHONE (Include Area Code)
603-646-4100

22c. OFFICE SYMBOL
CECRL-EC

PREFACE

This report was prepared by Dr. Yin-Chao Yen, Research Physical Scientist, of the Civil and Geotechnical Engineering Research Branch, Experimental Engineering Division, U.S. Army Cold Regions Research and Engineering Laboratory. Funding for this research was provided by DA Project 4A161102AT24, *Research in Snow, Ice and Frozen Ground*, Task SS, *Properties of Cold Regions Materials*, Work Unit 021, *Synopsis of Cold Regions Environmental Heat Transfer.*

Dr. Virgil Lunardini and Dr. Yoshisuke Nakano of CRREL technically reviewed the manuscript of this report.

The contents of this report are not to be used for advertising or promotional purposes. Citation of brand names does not constitute an official endorsement or approval of the use of such commercial products.

CONTENTS

ILLUSTRATIONS

TABLES

NOMENCLATURE

a	constant in eq 16
A	cross-sectional area
b	fissure width, also constant in eq 16
B	constant in eq 6, 7 and 8
$a+b$	fissure-to-fissure spacing
d	diameter of sphere
D	diameter of conduit
D_p	nominal particle diameter
f	friction factor defined as $2g_c D(-\Delta p)_f \varrho / LG^2$
f_p	friction factor for porous media defined as $\dfrac{2g_c D(-\Delta p)_f \varrho}{F_f L G^2}$
f'_p	friction factor defined in eq 18
F_f	friction factor coefficient
F_{Re}	Reynolds number factor
g	gravitational constant
g_c	conversion factor
G	mass flow rate
L	sample length
lw_f	frictional losses per unit mass
N	number of tubes, in cross-sectional area A
p	pressure
$(-\Delta p)_f$	pressure drop due to friction losses
r_0	radius of capillary tube
Re	Reynolds number defined as $D\varrho u/\mu$
Re_l	local pore Reynolds number
Re_p	Reynolds number for porous media defined as $D_p \varrho v F_{Re}/\mu$
Re′	Reynolds number defined in eq 19
x,y,z	Cartesian coordinates
u	velocity component in x-direction
v	velocity component in y-direction
w	velocity component in z-direction
μ	viscosity
ϱ	density
ϵ, ϵ_0	porosity, highest porosity
δ	surface roughness
γ	correlation coefficient
ψ	sphericity

On the Pressure Drop Through a Uniform Snow Layer

YIN-CHAO YEN

INTRODUCTION

Fluid flow through a bed of contiguous particles is distinct from the flow through a conduit. Since its passage is between the particles of the bed, the flow is dependent upon the porosity of the bed or column and diameter, sphericity, orientation and roughness of the particles. The actual linear velocity of the fluid through the passages in the porous medium may be expressed in terms of "superficial" velocity (computed as the rate of flow of fluid through the entire undisturbed cross-sectional area of the bed).

The most frequently used model for volume-averaged flow through a porous medium is Darcy's flow model. In one-dimensional flow, it can be expressed by

$$u = \frac{K}{\mu} \frac{\partial p}{\partial x} \tag{1}$$

where u = velocity component in x-direction
K = permeability of the medium
μ = viscosity
p = pressure.

For three-dimensional flow in the presence of a gravitational acceleration vector $\mathbf{g}$ (g_x, g_y, g_z), eq 1 can be written as

$$\mathbf{v} = \frac{K}{\mu}(-\nabla p + \varrho \mathbf{g}) \tag{2}$$

where $\mathbf{v}$ is the velocity vector, ϱ is density and K, usually expressed in units of length squared (i.e. m^2, cm^2, or ft^2), can be determined by measuring the pressure drop and the flow rate. Considering the pores as a bundle of parallel capillary tubes of radius r_0 or the pores as a stack of parallel capillary fissures of width b and fissure-to-fissure spacing $a+b$, Bear (1972) derived the following expressions:

$$K = \frac{\pi r_0^4 N}{8A} \tag{3}$$

and

$$K = \frac{b^3}{12(a+b)} \tag{4}$$

where N is the number of tubes contained on a cross section of area A.

Kozeny (1927), on the other hand, considered the porous medium as a collection of solid spheres and arrived at the following permeability expression:

$$K \sim \frac{d^2 \epsilon^3}{(1-\epsilon)^2} \tag{5}$$

where ϵ is the porosity (the ratio of void volume to the total volume of the porous medium), and d is the diameter of the spheres. Darcy's flow model is believed to be valid as long as the so-called local pore Reynolds number Re_l based on local volume-averaged speed [i.e. $(u^2+v^2+w^2)^{1/2}$] and $K^{1/2}$ are smaller than one. For Re_l greater than one, modification of this model has been proposed by Forschheimer (1901) as

$$-\frac{\partial p}{\partial x} = \frac{\mu}{K} u + B \varrho u^2. \tag{6}$$

For three dimensions and in the presence of body acceleration, this modification becomes

$$\mathbf{v} + \frac{BeK}{\mu} |\mathbf{v}| \mathbf{v} = \frac{K}{\mu}(-\nabla p + \varrho \mathbf{g}). \tag{7}$$

Ward (1964) suggested the value of B as

$$B = -0.55 K^{1/2}. \tag{8}$$

for Re_l exceeding approximately 10. Ergum (1952), after conducting extensive measurements on gas flow through columns of packed spheres, sands and pulverized coal, provided the correlations for K and B as

$$K = \frac{d^2\epsilon^3}{150(1-\epsilon)^2} \tag{9}$$

and

$$B = \frac{1.75(1-\epsilon)}{d\epsilon^3} \tag{10}$$

The loss due to friction accompanying the flow through porous media can be derived from expressions used for fluid flow through conduits such as

$$f = \frac{2g_c D lw_f}{L v^2} = \phi\left[\left(\frac{\delta}{D}\right)\left(\frac{D\varrho u}{\mu}\right)\right] \tag{11}$$

where f = frictional loss factor
g_c = conversion factor (32.17 poundals per pound in English units)
D = diameter of the conduit
L = length of the conduit
lw_f = frictional energy loss per unit mass
δ = surface roughness
u = superficial velocity, i.e. a linear velocity computed on the basis of the total crosssectional area.

In the case of fluid flow through a porous medium, the Reynolds number will be modified to

$$\mathrm{Re_p} = \frac{D_p \varrho u F_{Re}}{\mu} \tag{12}$$

where D_p is the diameter of the particle, F_{Re} is a factor dependent on the value of porosity ϵ and sphericity ψ (which is defined as the area of the sphere having the same volume as the particle divided by the area of the particle) of the medium. The friction factor f_p is adjusted to include a factor F_f also dependent on the values of ϵ and ψ as

$$f_p = \frac{2g_c D_p lw_f}{Lv^2 F_f} = \frac{2g_c D_p(-\Delta p)_f\,\varrho}{F_f L G^2}. \tag{13}$$

When all particles are of the same size, the screen size (D_{avg}) may be used. For mixed sizes, D_p is the mean surface diameter given by

$$D_p = \left[\frac{\Sigma M_i/D_i}{\Sigma M_i/D_i^3}\right]^{1/2} \tag{14}$$

where M_i is the mass fraction of a given particle size and D_i is the diameter of particles in each size fraction taken as the arithmetic average of the screen openings passing and retaining the particles. The value of F_{Re} and F_f can be evaluated from the graph given in Brown et al. (1953) and presented as functions of ϵ and ψ. The porosity is closely related to the sphericity. However, different porosities are expected with particles of the same shape through variations in spatial arrangement. Consequently both porosity and sphericity are required to define the porous medium. Although the sphericity could theoretically be calculated from the dimensions of the particle, this is often difficult or virtually impossible for randomly packed beds of uniform-sized particles. The sphericity is found to be a unique function of porosity with a slight variation due to the nature of packing (i.e. loose, normal or dense).

EXPERIMENTAL SETUP AND PROCEDURE

The test apparatus is identical to the one used in determining the effective thermal conductivity and water vapor diffusivity of the snow (Yen 1962, 1963). Figure 1 is a schematic of the experimental setup. The entire apparatus, with the exception of the manometer, the wet-test meter (to measure the air flow rate) and the Leeds and Northrup potentiometer (placed in the adjacent corridor maintained at ordinary room temperature), was situated in a refrigerated room kept at approximately -20°C. Coldroom air was compressed and then passed through a tank to minimize the fluctuations of the air pressure. A pancake-type pressure regulator was used to obtain the desired flow rate. Since the coldroom could only be maintained to within ±1°C, the air was passed through a constant temperature bath where the temperature could be maintained at slightly above room temperature to an accuracy of ±0.05°C.

The Dewar flask, 6.5 cm I.D., 15.24 cm in height and made of double-walled glass tubing with the annular space being evacuated and the internal surface plated with silver, contained the snow sample and was enclosed in an aluminum casing equipped with a flange at both ends. The casing was made so that the flask fitted tightly into it, and the flask was coated with a low-temperature silicone grease before assembly to prevent any possible air leakage. As soon as a steady state was established, the water temperature at the wet-test meter was recorded with a Rubican potentiometer

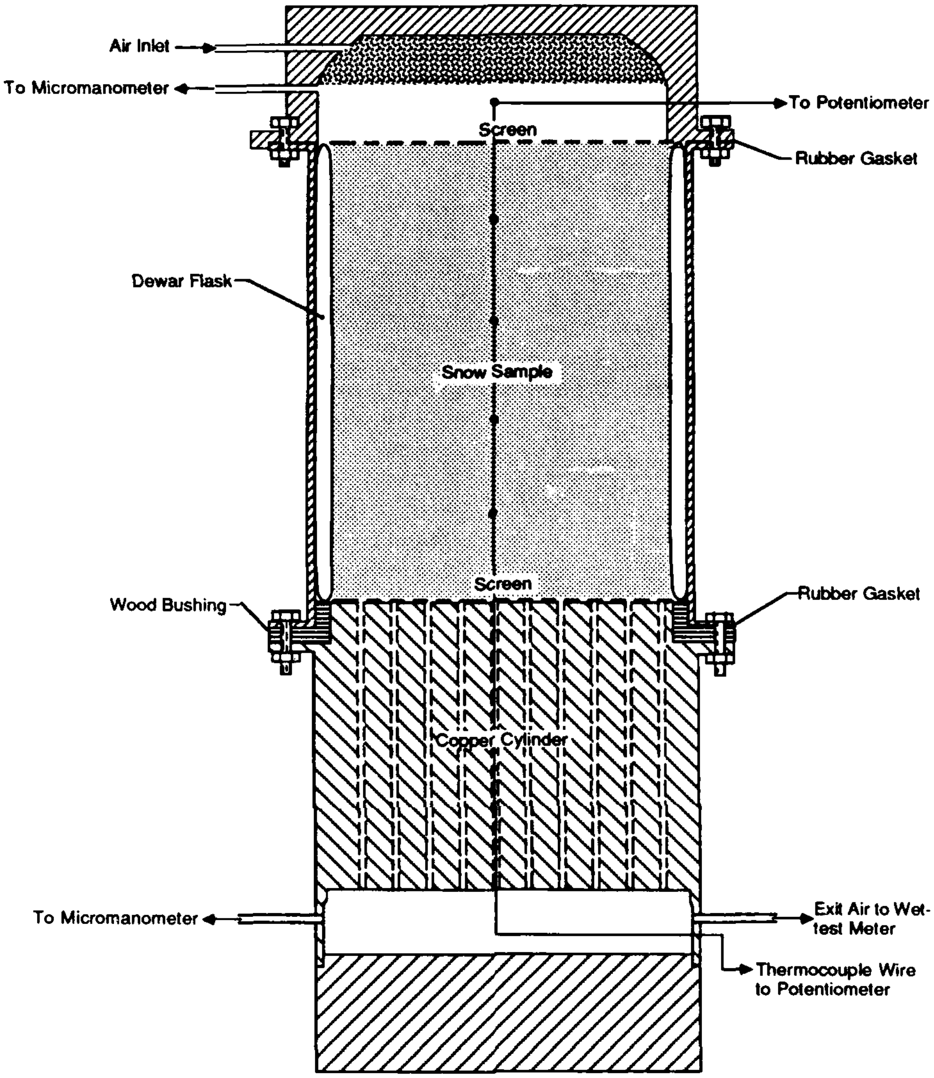

Figure 1. Schematic of the experimental setup.

accurate to ±0.05°C along with the absolute barometric pressure. The wet-test meter was checked by the standard displacement method and was found to be accurate within 20 cm^3 out of 3000 cm^3 (±0.7%). The displacement capacity of the meter is 300 cm^3 per revolution with 300 divisions on the dial. The snow samples for the experiments covered a range of sieve numbers, 5–10, 10–12, 14–16, 18–20 and 25–30, with corresponding nominal snow particle diameters of 0.219, 0.182, 0.129, 0.092 and 0.065 cm, respectively. The snow sample density was determined by recording the amount of snow poured into the flask to be flush with the sample container (i.e. ϱ_s = weight of snow/volume of the sample container). Several determinations were made for all the specific sieve fractions and an arithmetic average snow density was determined.

EXPERIMENTAL RESULTS

A great number of experimental runs were conducted for each snow density covered in the study.

Table 1. Summary of derived parameters as a function of snow density.

Snow density, ϱ_s (g/cm³)	Snow porosity, ϵ	Snow particle diameter, D_p (cm)	Sphericity of snow particle, ψ	Reynolds number factor, F_{Re}	Friction coefficient, F_f
0.377	0.589	0.219	0.55	43.5	830
0.387	0.578	0.182	0.55	45.0	950
0.427	0.534	0.129	0.60	47.0	1150
0.447	0.512	0.092	0.65	47.0	1150
0.472	0.485	0.065	0.70	47.0	1150

Table 1 summarizes the derived parameters as function of snow density. The porosity ϵ is evaluated as

$$\epsilon = \frac{\varrho_i - \varrho_s}{\varrho_i} \tag{15}$$

where ϱ_i is the ice density, usually taking a value of 0.917 g/cm³. The snow particle nominal diameter D_p was evaluated by arithmetically averaging the two sieve openings. The sphericity ψ, Reynolds number factor F_{Re} and coefficient F_f are taken from the graphs given in Brown et al. (1953). Since the snow density has only slightly more than 25% variation, there is merely a weak variation at the most in values of ψ and F_{Re}. However, the values of F_f were rather sensitive to the changes of ϵ and ψ. Figures 2a and b show the variation of pressure drop $(-\Delta p)_f$ vs the mass flow rate G (g/cm²-s). It can be seen that under the combination of experimental conditions (i.e. for the range of snow density and the variation of the mass flow rate covered in this study) a linear relationship exists between $(-\Delta p)_f$ and G. The coefficients a and b of the linear expression

$$(-\Delta p)_f = a + b\,G \times 10^{-4} \tag{16}$$

were determined from least-squares analysis and are summarized in Table 2 along with the correlation coefficients. Theoretically, the values of a should be zero, and small values of a are indicative of the accuracy of the experimental measurement. However, for practical purposes, one can hardly

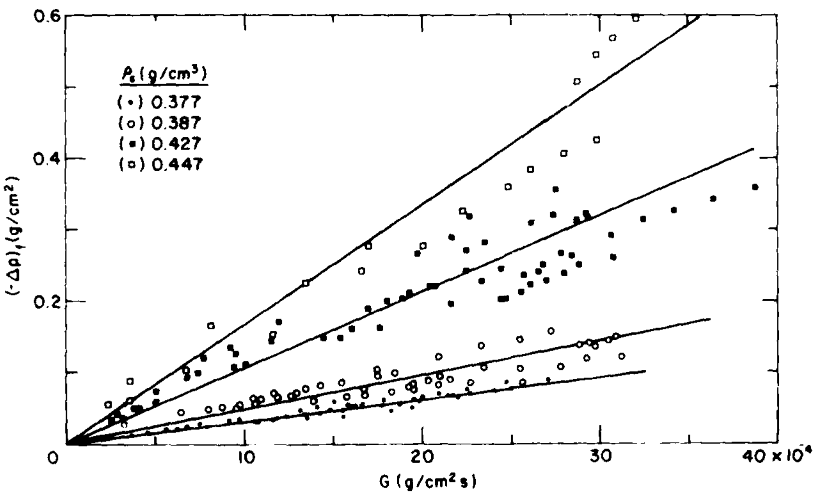

a. For ϱ_s = 0.377, 0.387, 0.427 and 0.447 g/cm³.

Figure 2. Pressure drop due to friction losses as a function of mass flow rate G.

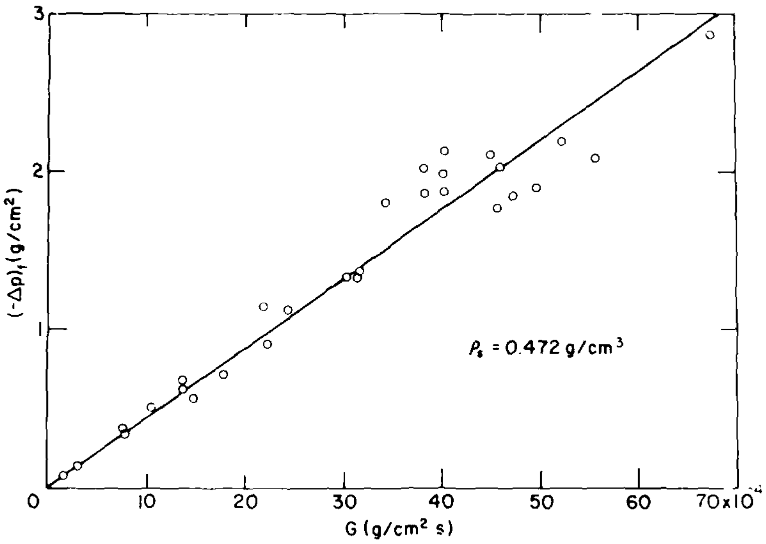

b. For ϱ_s = 0.472 g/cm³.

Figure 2 (cont'd).

Table 2. Coefficients *a* and *b* in $(-\Delta p)_f = a + bG \times 10^{-4}$ and coerrelation coefficient γ.

Snow density, ϱ_s (g/cm³)	Coefficient a (gf*/cm²)	Coefficient b (gf•s/g)	Correlation coefficient, γ
0.377	3.671×10^{-4}	31.267	0.9492
0.387	1.582×10^{-2}	39.382	0.8130
0.427	3.137×10^{-2}	88.425	0.8681
0.447	8.854×10^{-3}	176.95	0.9933
0.472	8.478×10^{-2}	413.20	0.9504

* gf—gram-force.

detect that the lines in Figures 2a and b do not pass through the origin.

Table 3 summarizes the experimental data and the calculated values of Re_p (defined as D_pGF_{Re}/μ) and friction factor f_p [defined in eq 15 as $f_p = 2g_cD_p(-\Delta p)_f\varrho/F_fLG^2$]. An average value of μ based on the arithmetic mean of the inlet and outlet air temperature was used. The mass flow rate was determined on the basis of the exit air temperature and the prevailing atmospheric pressure. Figure 3 shows the variation of f_p versus Re_p. The results of a least-squares analysis of the results can be expressed by

$$f_p = \frac{118}{Re_p^{1.095}} \tag{17}$$

with a rather high correlation coefficient of 0.9688. Equation 17 gives a value of f_p approaching that of $f_p = 65/Re_p$ as Re_p approaches the limit of the laminar flow region (say $Re_p = 400$) recommended for randomly packed particles (metallic or nonmetallic cylinders, rings, spheres, etc.).

Another way to represent the experimental results is by expressing the friction factor f_p' and the Reynolds number Re_p', respectively, by

$$f_p' = \frac{f_pF_f\epsilon^3}{2(1-\epsilon)} \tag{18}$$

and

$$Re_p' = \frac{Re_p}{F_{Re}(1-\epsilon)} \, . \tag{19}$$

The least-squares analysis of f_p' and Re_p' can be represented by

$$f_p' = \frac{Re_p}{Re_p'^{0.9093}} \tag{20}$$

but only with a moderate correlation coefficient of 0.8385. Figure 4 shows a plot of f_p' vs Re_p', and it can be clearly seen that the value f_p' has a weak dependence on the snow density or porosity.

Table 3. Summary of experimental results and calculated data.

$G \times 10^{-4}$ $(g/cm^2\ s)$	$(-\Delta p)_f$ (gf/cm^2)	Re $(D_p F_{Re} G/\mu)$	f_p $[2g_c D_p (-\Delta p)_f \varrho / F_f L G^2]$
$\varrho_s = 0.377\ g/cm^3$, $D_p = 0.219\ cm$			
13.11	0.048	75.1	1.28
14.02	0.051	80.3	1.19
9.11	0.032	52.2	1.77
7.57	0.027	43.3	2.16
15.09	0.051	86.4	1.03
16.20	0.053	92.8	0.92
17.80	0.062	102.0	0.90
19.52	0.062	112.0	0.74
24.70	0.085	142.1	0.64
27.09	0.088	155.7	0.55
25.09	0.078	144.2	0.57
22.68	0.070	130.4	0.62
21.47	0.068	123.5	0.68
19.98	0.067	114.9	0.77
5.66	0.019	32.4	2.72
9.70	0.033	55.6	1.61
11.63	0.034	66.6	1.15
14.14	0.041	81.0	0.94
15.82	0.052	90.9	0.95
19.77	0.057	113.5	0.67
21.75	0.068	124.8	0.66
24.02	0.075	137.9	0.59
21.91	0.066	125.9	0.63
10.61	0.031	60.9	1.26
3.71	0.012	21.3	4.00
6.84	0.024	39.1	2.35
16.60	0.058	95.0	0.96
17.70	0.055	101.3	0.80
20.93	0.070	119.8	0.73
22.57	0.075	129.1	0.67
16.02	0.051	91.7	0.91
14.70	0.047	84.0	1.00
13.29	0.042	75.9	1.08
18.36	0.054	105.2	0.73
6.23	0.022	35.7	2.60
7.86	0.024	45.1	1.78
10.70	0.029	61.5	1.16
12.34	0.038	70.9	1.14
15.45	0.047	89.0	0.90
11.70	0.035	67.3	1.17
4.66	0.015	26.7	3.17
13.36	0.037	76.9	0.95
15.54	0.038	89.4	0.72
18.20	0.046	104.9	0.64
19.39	0.051	111.8	0.62
$\varrho_s = 0.387\ g/cm^3$, $D_p = 0.182\ cm$			
9.70	0.053	47.8	1.88
10.69	0.056	52.7	1.63
12.92	0.070	63.8	1.40
28.83	0.137	142.7	0.55
29.43	0.142	145.6	0.55
30.48	0.144	150.9	0.52
23.49	0.107	116.2	0.65
13.89	0.060	68.8	1.04
16.73	0.069	82.7	0.82
19.43	0.075	95.9	0.66
20.94	0.096	103.5	0.73
29.20	0.118	144.5	0.46
25.50	0.105	126.2	0.54
31.16	0.123	154.2	0.42
20.92	0.083	103.4	0.63
25.65	0.081	125.9	0.41
8.77	0.051	43.2	2.21
9.67	0.051	47.6	1.81
10.73	0.061	52.9	1.77
12.59	0.068	62.1	1.43
30.93	0.150	153.0	0.52
29.72	0.135	147.1	0.51
21.50	0.091	106.3	0.66
20.26	0.089	100.2	0.72
19.46	0.083	96.3	0.73
19.33	0.081	95.5	0.72
18.33	0.077	90.6	0.76
16.84	0.072	83.2	0.85
15.94	0.066	78.8	0.86
27.80	0.106	137.6	0.46
22.72	0.088	112.3	0.57
17.50	0.102	86.0	1.11
20.93	0.123	86.5	0.94
23.27	0.137	115.0	0.84
25.54	0.145	126.3	0.74
27.27	0.157	134.9	0.70
11.75	0.070	57.8	1.69
14.24	0.083	70.2	1.36
15.41	0.085	71.5	1.19
17.52	0.096	86.2	1.04
18.20	0.100	89.8	1.01
6.39	0.044	31.5	3.60
8.00	0.048	39.4	2.50
10.43	0.063	42.8	1.93
11.89	0.065	48.8	1.53
3.39	0.026	16.7	7.56
13.41	0.076	66.1	1.41
$\varrho_s = 0.427\ g/cm^3$, $D_p = 0.129\ cm$			
3.84	0.050	14.1	6.63
16.95	0.190	62.5	1.29
9.48	0.107	34.9	2.33
4.11	0.050	15.1	5.77
5.00	0.059	18.3	4.61
2.48	0.034	9.1	10.82
18.04	0.201	66.6	1.21
10.16	0.110	37.4	2.08
24.38	0.246	90.1	0.81
16.02	0.160	59.1	1.22
2.91	0.041	10.7	9.47
28.43	0.262	105.0	0.63
26.52	0.240	98.1	0.67
21.64	0.198	79.9	0.83
11.54	0.144	42.5	2.11
7.39	0.099	27.1	3.55

Table 3 (cont'd).

$G \times 10^{-4}$ ($g/cm^2\ s$)	$(-\Delta p)_f$ (gf/cm^2)	Re ($D_p F_{Re} G/\mu$)	f_p [$2g_c D_p(-\Delta p)_f \rho / F_f L G^2$]
5.02	0.074	18.4	5.73
9.52	0.127	35.0	2.74
29.18	0.319	107.8	0.73
22.57	0.243	83.3	0.93
19.32	0.211	71.2	1.11
34.16	0.327	126.3	0.55
30.59	0.290	113.0	0.61
27.75	0.265	102.5	0.67
14.43	0.149	53.2	1.40
15.43	0.150	56.9	1.23
25.50	0.212	94.2	0.64
26.98	0.226	99.7	0.61
24.68	0.202	91.2	0.65
6.90	0.096	25.4	3.94
22.68	0.321	83.8	1.22
9.19	0.135	33.8	3.12
11.91	0.172	43.9	2.37
7.98	0.121	29.4	3.71
19.77	0.266	73.0	1.33
21.74	0.290	80.3	1.20
27.53	0.357	101.8	0.92
22.46	0.271	83.0	1.05
23.41	0.283	86.5	1.01
26.10	0.310	96.6	0.89
27.37	0.320	101.3	0.84
28.64	0.311	106.0	0.74
29.31	0.316	108.5	0.72
32.42	0.313	120.1	0.58
36.38	0.340	134.8	0.50
38.82	0.358	144.0	0.46
26.10	0.221	96.6	0.63
20.61	0.219	76.2	1.01
3.02	0.035	11.1	7.50
18.97	0.202	70.1	1.10
20.60	0.220	76.2	1.01
23.36	0.228	86.4	0.82
17.68	0.164	65.3	1.03
25.68	0.236	95.1	0.70
26.73	0.248	99.0	0.68
28.09	0.238	104.0	0.59
28.82	0.250	106.7	0.59
30.94	0.258	114.5	0.53
24.60	0.201	91.0	0.65

$G \times 10^{-4}$ ($g/cm^2\ s$)	$(-\Delta p)_f$ (gf/cm^2)	Re ($D_p F_{Re} G/\mu$)	f_p [$2g_c D_p(-\Delta p)_f \rho / F_f L G^2$]
ϱ_s = 0.447 g/cm³, D_p = 0.092 cm			
2.38	0.053	6.2	13.05
3.59	0.089	9.3	9.62
8.00	0.166	20.8	3.60
32.03	0.599	83.8	0.81
30.71	0.566	80.3	0.83
29.87	0.544	78.2	0.84
28.64	0.507	75.0	0.86
24.82	0.425	64.9	0.96
13.34	0.224	34.8	1.75
16.93	0.281	44.2	1.37
ϱ_s = 0.472 g/cm³, D_p = 0.065 cm			
7.79	0.379	14.3	6.13
13.68	0.667	25.2	3.50
24.30	1.120	44.8	1.86
13.70	0.617	25.2	3.23
22.31	0.909	41.1	1.79
14.60	0.553	26.9	2.55
2.84	0.140	5.2	17.06
1.62	0.098	3.0	36.89
21.78	1.142	40.2	2.36
34.31	1.755	63.5	1.46
40.89	2.122	75.7	1.25
40.75	2.016	75.4	1.19
38.14	1.871	70.6	1.26
10.41	0.526	19.1	4.77
44.89	2.098	83.1	1.02
42.66	1.976	79.0	1.07
40.72	1.868	75.4	1.11
7.65	0.364	14.1	6.10
45.72	2.020	84.7	0.95
30.26	1.320	56.0	1.42
31.10	1.326	57.5	1.35
31.58	1.348	58.4	1.33
67.45	2.862	125.2	0.62
52.32	2.175	97.1	0.78
17.90	0.710	33.0	2.18
47.02	1.828	87.1	0.81
45.59	1.753	84.5	0.83
49.67	1.879	92.0	0.75
55.40	2.066	102.8	0.66

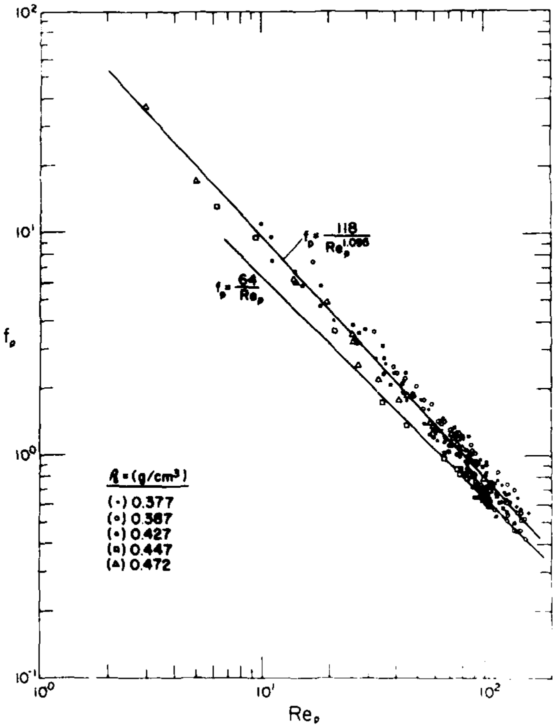

Figure 3. Relationship between friction factor f_p *and Reynolds number* Re_p.

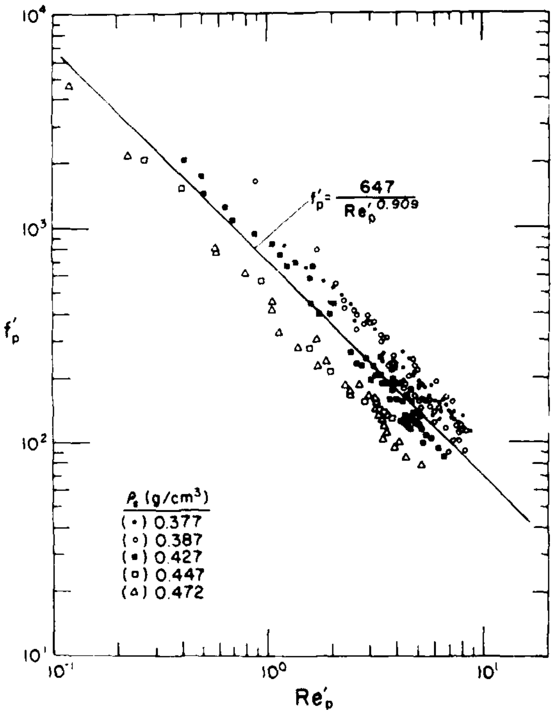

Figure 4. Relationship between friction factor f'_p *and Reynolds number* Re'_p.

DISCUSSION AND CONCLUSIONS

As shown in Table 2, the pressure drop through the snow layer for snow with density ranging from 0.377 to 0.472 g/cm³ can be fairly well represented linearly with the superficial mass flow rate G. The least-squares analysis for each snow density resulted in correlation coefficients from a moderate value of 0.8130 to a rather high value of 0.9933. From Figure 3, it can be seen that the air flow encounters higher resistance through snow as compared to gas flow through randomly packed porous columns of metallic and nonmetallic spherical and nonspherical materials (in the latter case, there was no phase change or mass transport accompanying the flow). Since snow is very sensitive to temperature, its physical properties are constantly changing through metamorphism, which creates ice bonds among the snow grains even under isothermal conditions through the process of sintering.

Since the experiment was set up to evaluate the thermal conductivity and vapor diffusivity of the snow, a moderate temperature gradient was imposed, even though the air entering at the top of the column was saturated to prevent or to limit the mass transport between the snow grains and the fluid stream as it flowed through the interconnected pores. Though a thermal equilibrium is assumed between the snow grain and the air stream as it passes the grain surface, the air still picks up the water vapor as it flows downward and comes into contact with snow, which was maintained at higher temperature at the exit. The moist snow must exhibit more drag or stickiness to the air flow than the dry and rather smooth surfaces of metallic and nonmetallic surfaces.

In laminar flow, equations of the same form may be used for the friction loss through the porous medium as for the fluid flow through the conduits (i.e. the pressure drop due to friction losses through a porous medium) is

$$(-\Delta p)_f = \frac{32 L v \mu F_f}{g_c D_p^2 F_{Re}} = \varrho l w_f \tag{21}$$

and for flow through a conduit is

$$(-\Delta p)_f = \frac{32 L v \mu}{g_c D^2} = \varrho l w_f . \tag{22}$$

In both flows, the friction factor can be represented by

$$f_p = \frac{64}{Re_p}, \quad f = \frac{64}{Re} . \tag{23}$$

The only difference between f_p, Re_p and f, Re is that f_p and Re_p contain factors of F_f and F_{Re}, respectively, in addition to the parameters used in defining f and Re. By rewriting eq 21, i.e. by solving for velocity u, it follows that

$$u = \frac{g_c D_p^2 F_{Re}}{32 F_f} \frac{\varrho l w_f}{L \mu} = K \frac{\varrho l w_f}{L \mu} \tag{24}$$

in which K is the air permeability of snow used in eq 1, i.e.

$$K = \frac{g_c D_p^2 F_{Re}}{32 F_f} . \tag{25}$$

From this, the value of K can be calculated without performing an experiment, if the dimensionless factors F_{Re} and F_f and the particle dimensions are known. The value of K is directly proportional to D_p^2 but implicitly K depends on porosity and sphericity through the factors of F_{Re} and F_f.

Bender (1957) reported an extensive study on air permeability of snow and pointed out that the air flow is laminar for velocities of less than 5 cm/s for fine-grained snow (less than 0.8 mm in diameter); 2 cm/s for medium-grained snow (0.8 to 1.2 mm in diameter); and 1 cm/s for large-grained snow. He reported that all of his results, as long as the flow is in laminar region, can be represented by a single relationship, i.e.

$$K = \frac{16.8 D_p^{1.63} \epsilon \epsilon_0}{\epsilon_0 - \epsilon} \tag{26}$$

where K = air permeability expressed in cm/s
D_p = average snow grain size in mm
ϵ_0 = highest porosity (i.e. when the packing is in loosest state) attainable for the given shape of the snow particle.

Since no specific experimental data were given in terms of pressure gradient, volumetric flow rate or superficial velocity, or porosities ϵ and ϵ_0, it was not possible to compare the results from eq 25 and 26. Furthermore, snow is so sensitive to the temperature and aging through metamorphism that it will be indeed difficult to reproduce experimental results even if identical samples and measurement techniques are used.

It can be concluded from this study that the pressure drop or friction loss of air flow through a uniform snow layer can be correlated in terms of f_p and Re_p with a high correlation coefficient (0.9688) or in modified form of f_f' and Re_p' with a moderate correlation coefficient of 0.8385. In view of the complex processes of mass exchange and physical structure transformation taking place even under isothermal conditions, the results presented should provide useful information in predicting energy requirements for air to penetrate a uniform snow layer of various snow densities.

LITERATURE CITED

Bear, J. (1972) *Dynamics of Fluid in Porous Media*. New York: American Elsevier.

Bender, J.A. (1957) Air permeability of snow. USA Snow, Ice and Permafrost Research Establishment, Research Report 37. AD 158 193.

Brown, G.G. et al. (1913) *Unit Operations*. New York: John Wiley & Sons, fourth printing.

Ergum, S. (1952) Fluid flow through packed columns. *Chemical Engineering Progress*, **48**(2): 89-94.

Forschheimer, P.H. (1901) *Zeitschrift Ver. Dtsch. Ing.*, **45**: 1782-1788.

Kozeny, J. (1927) Uber kapillare Leitung des Wassers in Boden Sitzber. Akad. Wiss. Wien, *Math-Naturw. Kl.*, vol. 136, Abt IIa, p. 277.

Yen, Y.-C. (1962) Effective thermal conductivity of ventilated snow. *Journal of Geophysical Research*, **67**(3): 1091-1097.

Yen, Y.-C. (1964) Heat transfer by vapor transfer in ventilated snow. *Journal of Geophysical Research*, **68**(4): 1093-1101.

☆U.S. GOVERNMENT PRINTING OFFICE 1988-600-057/82039

A facsimile catalog card in Library of Congress MARC format is reproduced below.

Yen, Yin-Chao
On the pressure drop through a uniform snow layer / by Yin-Chao Yen. Hanover, N.H.: U.S. Army Cold Regions Research and Engineering Laboratory; Springfield, Va.: available from National Technical Information Service, 1988.
iv, 17 p., illus.; 28 cm. (CRREL Report 88-14.)
Bibliography: p. 10.
1. Fluid flow. 2. Friction coefficient. 3. Porous media. 4. Pressure. 5. Snow. I. United States Army. Corps of Engineers. II. Cold Regions Research and Engineering Laboratory. III. Series: CRREL Report 88-14.